A Node-Based Optimization Model with an Asymmetric Cost Function for Multi-Trolley Pose in Tunnel Lining to Minimize Concrete Consumption

Bingtao Chang, Zhigang Du, Zhijun Li, Junnan Feng, Jiahuan Ran and Wuming Zhang, China

Key words: tunnel lining, concrete minimization, trolley pose optimization, node-based model; digital construction

1. SUMMARY

Concrete consumption is a primary cost driver in tunnel secondary lining construction. The highly irregular as-built surfaces of excavated tunnels, combined with traditional trolley positioning methods aimed at guaranteeing minimum thickness specifications, frequently results in significant concrete over-consumption. This paper presents an automated, multi-trolley pose optimization method that leverages high-precision as-built point cloud data to determine an optimal sequence of trolley poses that minimizes total concrete usage. The methodology first involves rasterizing the tunnel point cloud data. Thin Plate Spline (TPS) interpolation is then employed to fill data voids, thereby generating a complete and seamless digital tunnel surface. Subsequently, a sequence of N trolleys, each modeled as a variable-radius frustum, is abstracted into a chain-like model connected by N+1 shared nodes. The state of each node is defined by its lateral offset (Y, Z) and its lining radius (R). This node-based model inherently ensures geometric continuity at the trolley joints. The optimization objective—to minimize the interstitial volume (i.e., the gap) between the tunnel surface and the trolley model—is formulated as a non-linear least-squares (NLS) problem and solved using the Ceres Solver library. A key innovation lies in the design of an Asymmetric Cost Function. This function applies a standard cost to concrete surplus (actual > design thickness), aligning with the primary goal of volume minimization. Conversely, it applies a high-weight penalty to any deficit (actual < design thickness). This strategy effectively transforms the rigid engineering constraint of minimum thickness into a robust, soft constraint within the optimization framework. The model flexibly accommodates various boundary conditions, including fixed-start, fixed-start-and-end, or fully adjustable node configurations. Experimental results demonstrate that the method converges rapidly to a set of globally optimized node parameters. A comparison of pre- and post-optimization concrete volumes, calculated precisely using a frustum-based model, confirms that the method achieves a significant reduction in concrete consumption (approx. 7.6%) while strictly adhering to all design specifications. This research provides a practical optimization tool for digital and automated tunnel construction, offering direct application value in reducing project costs and enhancing quality control.

A Node-Based Optimization Model with an Asymmetric Cost Function for Multi-Trolley Pose in Tunnel Lining to Minimize Concrete Consumption

Bingtao Chang, Zhigang Du, Zhijun Li, Junnan Feng, Jiahuan Ran and Wuming Zhang, China

In modern transportation and hydraulic engineering, tunnels serve as critical infrastructure for overcoming complex terrains and shortening transit distances, with their construction scale continuously increasing worldwide. During tunnel construction, the secondary lining is the most crucial component for ensuring long-term structural safety, waterproofing, and aesthetic quality(Zhou et al., 2023). Secondary lining typically employs large-scale steel mold trolleys for cast-in-place concrete construction. As concrete is the primary construction material for the secondary lining, its consumption directly dictates the direct economic costs of the project(Merisalu et al., 2023).

However, in practical engineering, the surface of tunnel excavation and primary support (referred to as the "as-built surface" or "excavated surface") exhibits extremely irregular and uneven characteristics due to the influence of surrounding rock geological conditions, blasting techniques, and mechanical construction errors(Ghorbani et al., 2020). To ensure that the secondary lining structure meets the Minimum Design Thickness required by design specifications at all locations, traditional construction methods often adopt a conservative "inclusive strategy," which involves increasing the redundancy of trolley positioning based on manual experience. While this approach avoids structural safety risks caused by insufficient thickness, it leads to significant "backfilling of over-excavation," resulting in enormous waste of concrete volume. In large-scale tunnel projects, the cumulative cost of excess concrete consumption resulting from even centimeter-level pose deviations is staggering(Manzoor et al., 2021). Therefore, how to utilize digital technology to precisely optimize trolley pose, minimizing concrete consumption while strictly adhering to the thickness baseline, has become an urgent problem demanding solution in green tunnel construction and refined construction practices(Hosamo and Hosamo, 2022; Khudhair et al., 2021).

With the development of mobile surveying technology and 3D Laser Scanning (LiDAR), utilizing high-precision point cloud data for tunnel quality assessment has become an industry standard. Currently, research by scholars domestically and internationally in the field of tunnel digitalization mainly focuses on the following three aspects:

First, in terms of tunnel point cloud processing and geometric inspection, researchers have proposed various algorithms to achieve point cloud denoising(Zhi et al., 2025), axis extraction(Kang et al., 2014), and automatic cross-section extraction(Xie et al., 2018) (such as RANSAC-based geometric fitting). These techniques provide the data foundation for obtaining high-precision tunnel "as-built" models. However, current inspection research mostly focuses on quality assessment after construction is completed, rather than real-time optimization guidance during the construction process.

Second, regarding trolley positioning and pose adjustment, traditional engineering practice relies on total stations combined with a few feature points for setting out. Although digital

positioning schemes based on BIM (Building Information Modeling) have emerged in recent years, most of these schemes only achieve spatial alignment between the trolley axis and the design axis, failing to fully consider the impact of the micro-undulations of the irregular surrounding rock surface on concrete volume(Shen et al., 2012). Existing "axis alignment" strategies often require overall translation or radius reduction when facing locally protruding rock walls, lacking local flexibility.

Finally, regarding the application of engineering optimization algorithms, Non-linear Least Squares (NLS) has been widely used in industrial vision and precision measurement(Suárez-Fino and Mayoral, 2024). However, in the field of tunnel trolley pose optimization, a critical bottleneck exists: the contradiction between the rigid minimum thickness constraint and the flexible objective of minimizing volume. Traditional symmetric objective functions (such as simply minimizing the sum of squared distances) cannot express the engineering red line that "thickness must absolutely not be less than 30cm" during the optimization process. Furthermore, when facing continuous construction with multiple trolleys, ensuring smooth transition (geometric continuity) at the joints is also a difficult problem that existing independent optimization algorithms have not solved well.

Addressing the aforementioned challenges, this paper proposes a collaborative optimization method for tunnel trolley pose based on a multi-node chain model and an asymmetric cost function. The research contributions of this paper are mainly reflected in the following aspects:

1. Node-based continuous optimization model: It breaks the limitations of independent single-trolley optimization. By abstracting continuous multiple trolleys into a chain model connected by shared nodes, it inherently ensures geometric smoothness at trolley joints.
2. Design of asymmetric cost function: Addressing the special constraints of tunnel engineering, an asymmetric cost function is designed. It transforms the rigid physical constraint of minimum thickness into an optimization objective with high-weight penalties, achieving a dynamic balance between quality safety and cost control.
3. High-precision rasterization and TPS interpolation preprocessing: A set of point cloud rasterization and hole-filling procedures suitable for irregular tunnel surfaces is proposed, ensuring the robustness of the optimization algorithm when dealing with complex as-built surface data.
4. Engineering value verification: Through verification with actual engineering data, it is proven that the algorithm can significantly reduce the concrete over-consumption rate while guaranteeing construction compliance, providing theoretical support and technical pathways for digitalized and refined tunnel construction.

The optimization scheme proposed in this paper primarily consists of three core stages. The first stage is data preprocessing, where massive discrete point clouds are transformed into continuous, complete rasterized surface models. Next is the geometric modeling stage, which establishes a node-based chain trolley model, converting complex pose adjustments into parameter solutions for a finite number of nodes. Finally, there is the non-linear optimization stage, utilizing an asymmetric cost function within the Ceres Solver framework to iteratively find the optimal volume solution that satisfies construction constraints.

3.1 Data Preprocessing and Surface Reconstruction

Due to the massive volume, unstructured nature, and existence of "data voids" caused by construction environment occlusions (e.g., ventilation ducts and supports) inherent in raw 3D scanned point clouds, direct application for spatial pose optimization results in extremely low computational efficiency and algorithmic instability. Therefore, it is imperative to transform the discrete geometric information into a continuous and regular mathematical surface.

3.1.1 Polar Parameterization and Rasterization

First, the point cloud in the three-dimensional Euclidean space is mapped to a parametric space referenced to the tunnel's design axis. Through projection transformation, each point is converted into a triplet comprising mileage L, polar angle θ, and radial distance R. To structure the discrete data, we subdivide the (L,θ) plane into a regular raster matrix with resolutions ΔL and $\Delta\theta$. Within each grid cell (i, j), the algorithm executes a minimum filtering strategy:

$$R_{i,j} = \min\{R|\ L \in [L_i, L_{i+1}), \theta \in [\theta_j, \theta_{j+1})\} \tag{1}$$

Retaining the minimum radial distance is significant because it represents the rock wall position that protrudes most toward the tunnel center within that local area. This step compresses the raw point cloud into an "angle-radius" raster map that records the "narrowest boundary," providing a conservative and safe geometric boundary for the subsequent evaluation of potential trolley interference.

3.1.2 Surface Completion via Thin Plate Spline

At actual engineering sites, scanning blind spots or occlusions result in numerous invalid values (voids) within the raster matrix. If left unaddressed, these voids will cause failures in volume integration during the optimization process. This paper introduces the Thin Plate Spline (TPS) interpolation algorithm for surface reconstruction of the raster map. The core principle of TPS is to find a mapping function $f(L,\theta)$ that minimizes the surface's Bending Energy while passing through all known grid points:

$$E(f) = \iint \left(\left(\frac{\partial^2 f}{\partial L^2} \right)^2 + 2\left(\frac{\partial^2 f}{\partial L \partial \theta} \right)^2 + \left(\frac{\partial^2 f}{\partial \theta^2} \right)^2 \right) dL d\theta \tag{2}$$

Compared to traditional linear interpolation, TPS generates a continuous, smooth surface with C^2 continuity through global optimization based on the spatial distribution of surrounding known points. This step not only fills missing data but also eliminates local distortions caused by isolated noise points, ultimately yielding a complete and intact as-built tunnel surface model $S_{tunnel}(L,\theta)$.

Through the aforementioned preprocessing, the irregular tunnel surface is successfully decoupled into a series of structured cross-section data. Each cross-section c corresponds to a radial sequence composed of *rn* sampling points. This structured data model provides a unified indexing basis for the spatial projection of the trolley model in subsequent Section 3.3 and the grid-point-based residual calculation in Section 3.4, ensuring a closed-loop and efficient data flow throughout the entire optimization process.

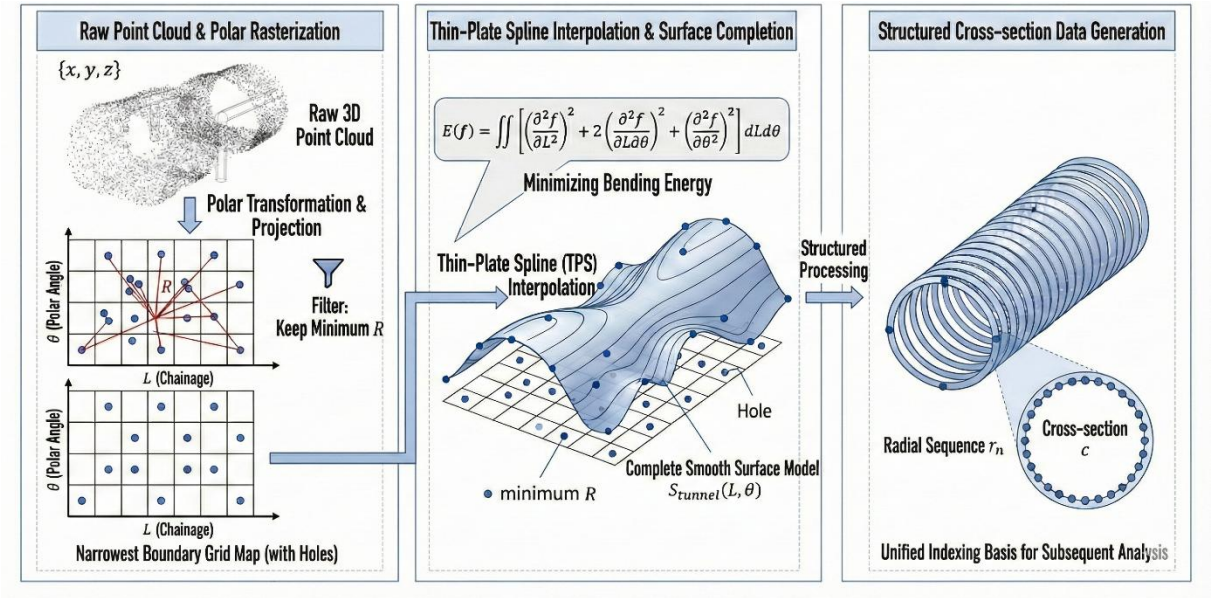

Figure 1. Schematic diagram of tunnel point cloud preprocessing and surface reconstruction principle.

3.2 Node-Based Multi-Trolley Chain Model

Traditional optimization for secondary lining construction usually treats a single trolley segment as an independent rigid body for adjustment. However, in continuous construction scenarios, this "isolated optimization" often leads to misalignment or radius mismatch at the joints between adjacent trolleys. This not only compromises the smoothness of the lining surface but also increases the risk of grout leakage. Therefore, this paper proposes a node-driven chain parametric model.

3.2.1 Node Parameterization and State Definition

We abstract continuous N trolleys into a dynamic chain connected by N+1 spatial nodes. The physical meaning of a node is the central control point of the start and end cross-sections of the trolley. For any node i , its state is defined by a three-dimensional parameter vector $\mathbf{P}_i$:

$$\mathbf{P}_i = [y_i, z_i, R_i]^T \tag{3}$$

Where (y_i, z_i) represent the horizontal and vertical displacement offsets of the node within the current mileage cross-section relative to the tunnel's design axis. R_i is the secondary lining trolley design radius at the cross-section where the node is located. Through this definition, the overall pose adjustment of the trolley is simplified into a coordinate search problem for a finite number of node vectors $\{\mathbf{P}_0, \mathbf{P}_1, \ldots, \mathbf{P}_N\}$.

3.2.2 Frustum Geometric Interpolation

In actual construction, the trolley is not a perfect cylinder; its radii at both ends and center position may have slight differences due to adapting to irregular surrounding rock. Therefore,

this paper models each trolley segment (located between node i and node i+1) as a variable-section frustum.

For any longitudinal position $t \in [0,1]$ (t is the scale factor relative to the trolley length) within the i-th trolley segment, its center trajectory $\mathbf{C}(t)$ and real-time radius $R(t)$ follow linear interpolation laws:

$$\mathbf{C}(t) = (1-t)\mathbf{P}_i^{yz} + t\mathbf{P}_{i+1}^{yz} \tag{4}$$

$$R(t) = (1-t)R_i + tR_{i+1} \tag{5}$$

This linear envelope model ensures that the trolley surface is geometrically differentiable and smooth. By utilizing this interpolation method, we can calculate the three-dimensional coordinates of any point on the trolley surface, thereby providing precise analytical expressions for calculating the "gap thickness" between the trolley and the tunnel surface reconstructed in Section 3.2 in the subsequent Section 3.4.

3.2.3 Joint Continuity and Boundary Constraints

The greatest advantage of the node-based model lies in its intrinsic geometric continuity constraint. Since the end of trolley i and the beginning of trolley i+1 share the same node parameter $\mathbf{P}_{i+1}$, the system can automatically ensure perfect closure of the center pose and cross-sectional radius at the joint without adding extra penalty terms during the optimization process.

Furthermore, this model possesses high boundary flexibility. In actual engineering, depending on the construction status of the start and end, we can achieve different engineering constraints by freezing specific parameter blocks:

Fixed-End: When a newly poured segment needs to align with an already completed lining, the starting node $\mathbf{P}_0$ is set as a constant.

Radius-Constrained: If the trolley's mechanical structure does not support variable radius, R_i can be set as globally consistent.

This node-based modeling approach successfully transforms the complex spatial surface matching problem into a parameter optimization problem with a compact topological structure and controllable degrees of freedom, laying the foundation for subsequent non-linear solving.

3.3 Optimization via Asymmetric Cost Function

The objective of this stage is to minimize the interstitial volume between the as-built tunnel surface S_{tunnel} and the trolley design surface $S_{trolley}$. This is not merely a simple geometric distance minimization problem but also a constrained optimization problem that includes a strict engineering safety baseline.

3.3.1 Discrete Formulation of the Objective

To calculate the concrete pouring volume, we transform the continuous volume integral into a numerical summation based on grid units. For each grid point (r,c), its actual concrete thickness $d(r,c)$ is defined as the difference between the radial distance of that point and the trolley's interpolated radius at that location.

Since the trolley is located inside the tunnel, the mathematical essence of the optimization is to make the trolley surface fit the tunnel surface as closely as possible without penetrating the rock wall (satisfying the minimum thickness). We model this process as a Non-linear Least Squares (NLS) problem, and its total cost function $F(\mathbf{P})$ is expressed as:

$$F(\mathbf{P}) = \sum_{c=1}^{cn} \sum_{r=1}^{rn} \rho\left(d(r,c) - d_{design}\right)^2 \tag{6}$$

Where d_{design} is the minimum secondary lining thickness required by specifications, and ρ is the asymmetric cost kernel function designed in this paper.

3.3.2 Asymmetric Cost Function Mechanism

In tunnel engineering, the physical consequences of "overfilling" and "underfilling" are vastly asymmetrical: exceeding the design thickness (surplus) only leads to material waste (economic loss), while being less than the design thickness (deficit) directly threatens structural safety (regulatory red line). Traditional symmetric cost functions (such as the L_2 norm) cannot express this difference, leading to optimization results that may violate regulations by causing "deficit" in some locations.

Therefore, this paper designs an asymmetric residual logic to weight the residual $\Delta d = d_{actual} - d_{design}$:

$$\rho(\Delta d) = \begin{cases} \Delta d, & \Delta d \geq 0 \quad \text{(Concrete surplus)} \\ w \cdot |\Delta d|, & \Delta d < 0 \quad \text{(Concrete deficit)} \end{cases} \tag{7}$$

Here, w is the penalty coefficient (in this paper, $w = 100$). This design causes the slope of the cost function to increase sharply when entering the "deficit zone," forming a high-gradient penalty barrier that forces the optimizer to prioritize adjusting the trolley pose to exit the non-compliant region, thereby refining the reduction of surplus volume while ensuring the lining thickness standard is met.

Due to the high non-linearity of the objective function involving coordinate transformations, trigonometric functions, and linear interpolation, we introduce the Google Ceres Solver(Agarwal et al., 2023) library and employ the Levenberg-Marquardt (LM) algorithm for solving.

4.1 Experimental Setup and Data Description

To verify the practical performance of the multi-trolley collaborative optimization algorithm proposed in this paper in a complex tunnel environment, this chapter selects a typical high-speed railway tunnel section under construction in Sichuan Province, China, as an experimental case. The geological conditions of this section are complex, and the surface of the initial support is significantly irregularly undulating due to blasting and shotcrete processes.

The experiment uses a 3D Laser Scanner (LiDAR) to conduct a full-field scan of the tunnel's inner wall after initial support. To simulate the real secondary lining construction environment, we strictly set the optimization geometric red lines according to the design drawings: simulating the continuous construction of 5 standard steel mold trolleys, each 12m long. The design radius of the inner surface of the secondary lining is 7.5m. According to engineering safety standards,

the absolute lower limit of the lining thickness is set to 30cm. This means that in the optimization calculation in Section 2.4, any sampling point with an actual thickness of less than 30cm will trigger a high-weight penalty. The "Fixed-Start" mode is set to simulate the engineering reality where the current 60m construction section needs to precisely connect with the completed lining section.

The optimization algorithm runs on a high-performance mobile workstation (Intel i7-12700H, 32GB RAM), and the software environment is developed based on C++13. To balance convergence accuracy and computational efficiency, the following hyperparameters are set for the algorithm in Section 2.4: Angular resolution ($\Delta\theta$): Raster circumferential sampling points rn = 300（corresponding to a physical spacing of approximately 0.16m）. Mileage resolution (ΔL)： Raster longitudinal step size *grid_resolution* = 0.2m. Asymmetric weight (w): Deficit penalty factor w is set to 100. The Levenberg-Marquardt algorithm of Ceres Solver is adopted, the linear solver is specified as DENSE_QR, the maximum number of iterations is set to 100, and the function convergence tolerance is set to 10^{-6} . Through the above settings, the experimental environment is strictly controlled within a framework consistent with engineering logic, ensuring the reliability and repeatability of the optimization results in Section 3.2.

4.2 Visual Analysis of Pose Adjustment

After the optimization calculation is completed, the algorithm outputs a sequence of globally optimal node parameters $\mathbf{P}_{opt}$. To verify its geometric validity, we re-project the optimized trolley model into the original 3D point cloud space and evaluate it from three dimensions: overall spatial alignment, typical cross-sectional fit, and joint continuity.

Figure 2(a) shows a global view of a typical tunnel cross-section. The solid black line represents the irregular as-built tunnel surface, and the dashed red line is the minimum thickness safety boundary (Safety Line) determined according to specifications. The blue dash-dotted line shows the traditional conservative initial pose. It can be seen that, to ensure the safety red line is not violated at any location (especially in the crown area), the initial pose is set conservatively, with its overall profile shrinking towards the tunnel center. Although this guarantees safety, it also results in a large gap between the trolley and the safety red line, indicating significant excess concrete consumption. The solid green line represents the trolley pose after optimization by the algorithm in this paper. By comparing with the initial pose, it is obvious that driven by the asymmetric cost function, the optimized trolley profile expands outward globally, closer to the red safety boundary. This expansion is not uniform, but adaptively adjusted according to the actual undulations of the as-built tunnel surface. In the overall view of Figure 2(a), the void space between the green curve (optimized pose) and the red curve (safety boundary) is significantly smaller than the area between the blue curve (initial pose) and the red curve. This close fit indicates that the algorithm successfully compressed unnecessary surplus volume on the entire cross-section, achieving a substantial improvement in overall conformity.

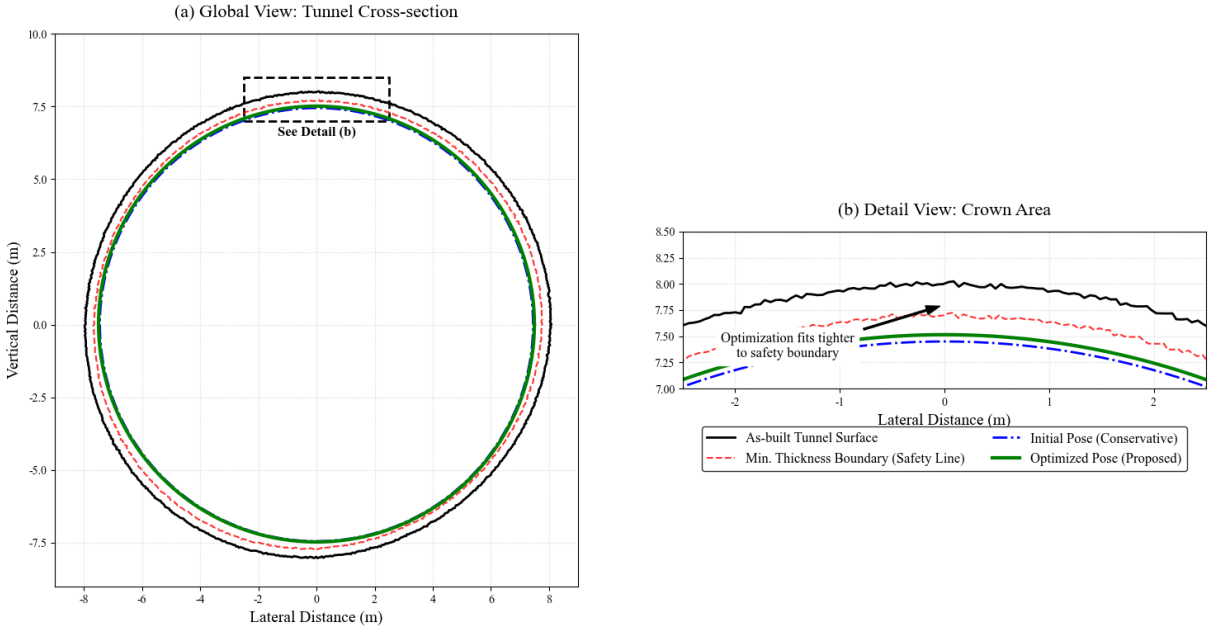

Figure 2. Comparison diagram of trolley pose optimization in a typical cross-section. (a) Global view of the tunnel cross-section, showing the as-built surface, safety red line, and trolley poses before and after optimization; (b) Zoomed-in view of the crown area, clearly showing that the optimized pose is closer to the safety boundary.

Figure 2(b) provides a detailed zoomed-in view of the crown area, which is typically a critical region for tunnel settlement control and ensuring secondary lining thickness. This figure clearly demonstrates how the asymmetric cost function guides fine adjustments of the trolley pose at a micro level. In Figure 2(b), the solid black line represents the irregular as-built surface, and the dashed red line is the rigid safety boundary 30cm from the as-built surface. We can observe that the blue initial conservative pose is positioned far from the safety boundary to avoid any potential risk of violating clearance, leading to a significant gap. In contrast, driven by the asymmetric cost function, the green optimized pose is "pushed" towards the safety boundary. As indicated by the black arrow in the figure, the optimized profile shifts upward and undergoes slight deformation, making it closely fit the red safety red line throughout the entire crown area. This adjustment strategy fully reflects the asymmetric characteristic of the cost function: when the trolley has not touched the red line, the optimizer tends to expand outward to minimize the gap (reducing the "surplus" cost); however, once approaching the red line, a high penalty for "deficit" becomes effective immediately, forming a solid barrier to prevent the trolley from crossing the red line. The final result is that the green curve is traced almost along the inner edge of the dashed red line, neither intruding into the restricted area nor leaving excessive wasted space, perfectly achieving ultimate optimization under safety constraints.

The core challenge of multi-trolley cooperative optimization lies in how to strictly ensure geometric closure at their physical connections while allowing each trolley segment to perform "personalized" pose adjustments according to local rock wall undulations. To verify the performance of the chain model proposed in this paper on this key indicator, we reconstructed the 3D trolley sequence morphology before and after optimization, as shown in Figure 3.

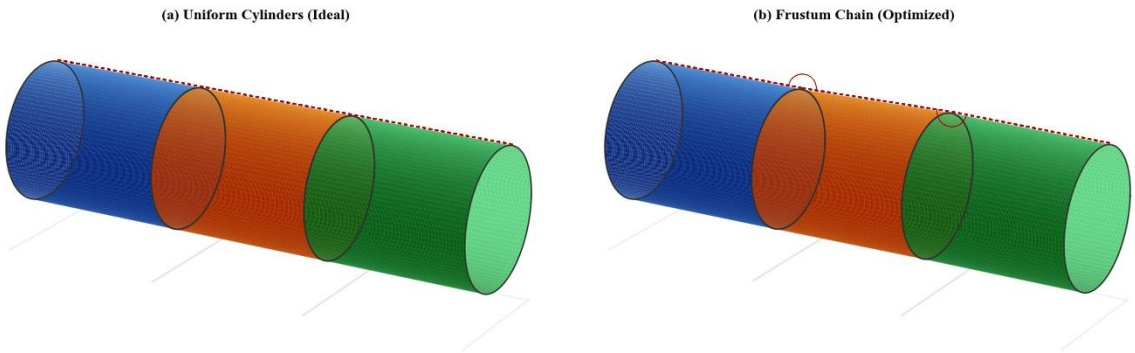

Figure 3: 3D comparison of trolley sequence geometric morphology. (a) Pre-optimization uniform cylindrical model, with segments rigidly aligned along the design axis; (b) Optimized frustum chain model, where segments have undergone adaptive deflection and diameter changes according to rock wall characteristics. Red circles highlight shared node joints between adjacent trolleys, confirming seamless connection under spatial deformation.

Figure 3(a) shows the traditional uniform cylindrical model (Uniform Cylinders). In this mode, the blue, orange, and green trolley segments are absolutely aligned along the design axis. Although the joints are flush, the overall morphology is rigid and cannot adapt to the actual non-linear undulations of the tunnel, leading to the aforementioned concrete overconsumption problem. Figure 3(b) shows the optimized model generated based on the algorithm in this paper. It can be clearly observed that to fit the irregular boundaries of the tunnel inner wall, each trolley segment (Frustum Segment) has undergone visible pose adjustments in space: Spatial deflection: The center axis of the trolley is no longer a straight line but forms a polyline adapted to the environment; Variable cross-section features: The start and end radii of each trolley segment are fine-tuned according to node parameters, exhibiting frustum features.

The areas highlighted by red circles in Figure 3(b) are critical for evaluating the success of the algorithm. Although adjacent trolley segments (e.g., the blue and orange segments) have undergone varying degrees of tilting and radius scaling, they maintain perfect geometric closure at the interface. Visual results confirm that the base surfaces of two adjacent frustums completely coincide in space, without any physical misalignment, steps, or gaps. This C^0 continuity (positional continuity) is mathematically enforced by the "shared node" topological structure described in Section 3.2—that is, node i is both the end point of segment i-1 and the start point of segment i. No matter how the optimization algorithm iteratively searches for node parameters $\mathbf{P}_i$, this topological constraint ensures the system will never "break". This geometric smoothness holds significant engineering value. In actual secondary lining construction, using independent optimization strategies easily leads to "stepping" phenomena between adjacent trolleys, which not only causes concrete grout leakage but also forms stress concentration points at joints, affecting the long-term waterproofing performance and bearing capacity of the lining structure. The chain model in this paper fundamentally avoids the aforementioned construction risks by eliminating geometric gaps, ensuring that the final formed tunnel secondary lining surface is flat, smooth, and structurally continuous.

4.3 Quantitative Evaluation of Concrete Savings

Subsequent to the qualitative visual analysis presented in Section 3.2, this section aims to assess the practical effectiveness of the multi-trolley collaborative optimization algorithm in

reducing concrete consumption through rigorous quantitative evaluations. The calculation of the total concrete volume is based on the continuous frustum chain model constructed in Section 3.2 and the as-built tunnel surface reconstructed in Section 3.1. By performing numerical integration of the differential volume between these two surfaces at the grid level (the methodology is detailed in Section 3.3.1), we accurately determined the theoretical required volumes for five trolley segments (totaling 60 meters) before and after optimization. The statistical results are presented in Table 1. The initial scheme employed a traditional "axis-aligned and radius-conservative" strategy to ensure against underbreak; whereas the optimized scheme utilizes the global optimal poses ($\mathbf{P}_{opt}$) output by the algorithm.

Table 1. Statistical Summary of Concrete Volumes Before and After Multi-Trolley Optimization (60m Test Section)

Trolley ID	Initial Volume (m^3)	Optimized Volume (m^3)	Volume Saved (m^3)	Saving Rate (%)
Segment1	185.4	172.1	13.3	7.17
Segment2	192.8	176.5	16.3	8.45
Segment3	188.2	175.8	12.4	6.59
Segment4	190.5	174.9	15.6	8.19
Segment5	187.9	173.6	14.3	7.61
Total	944.8	872.9	71.9	7.61

The data indicate that through multi-node collaborative optimization, the total concrete consumption for this 60-meter tunnel section decreased from 944.8 m^3 to 872.9 m^3, with a cumulative saved volume of 71.9 m^3, representing a significant overall saving rate of 7.61%. The saving rates for different segments fluctuated between 6.59% and 8.45%. This variation objectively reflects the uneven distribution of overbreak and underbreak in the surrounding tunnel rock. In areas where overbreak is more severe (such as Segment 2), the asymmetric cost function has greater optimization space to compress redundant volume, thereby achieving a higher saving rate. It must be emphasized that this 7.61% volume saving was achieved under the premise of strict compliance with safety specifications. Through validation of millions of grid points on the optimized model, the results show that the lining thickness at all points satisfied the rigid requirement of $d \geq 30cm$. This strongly proves the effectiveness of the asymmetric high-weight penalty mechanism described in Section 3.3.2 in preventing underbreak. In other words, the algorithm successfully "squeezed out" excess concrete within the safety boundaries, rather than compromising safety space to achieve cost reduction. For large-scale, long-distance tunnel projects, a material saving of nearly 8% signifies tremendous direct economic benefits and a reduction in carbon emissions, fully verifying the practical engineering value of the proposed algorithm.

Addressing the pervasive challenge of concrete over-consumption in tunnel secondary lining construction stemming from irregular as-built surfaces, this paper proposes and validates a collaborative trolley pose optimization method based on a multi-node chain model and an asymmetric cost function. Through theoretical derivation, algorithmic implementation, and empirical engineering studies, the following primary conclusions are drawn:(1) The innovatively designed asymmetric cost function successfully transforms the strict "minimum

thickness red line" of tunnel engineering into a high-potential penalty term within mathematical optimization. This enables the algorithm to maximize the compression of redundant space while rigorously adhering to the quality safety baseline, achieving a dynamic balance between safety constraints and the objective of volume minimization. (2) The proposed chain modeling approach based on shared nodes fundamentally resolves the common joint misalignment issue inherent in independent multi-trolley optimization from a topological perspective. Experimental results intuitively confirm that this model maintains perfect C^0 geometric continuity at adjacent trolley joints even under complex spatial pose adjustments, holding significant value for enhancing the aesthetic quality and waterproofing performance of the secondary lining. (3) Field test data indicate that when applied to a 60-meter complex tunnel section, the proposed method achieved a 7.61% reduction in concrete volume while ensuring lining thickness compliance across all areas. For large-scale tunnel projects, this saving rate translates into substantial reductions in direct economic costs and carbon emissions. In summary, this study provides a comprehensive digital solution for tunnel secondary lining construction, encompassing data acquisition, model construction, and optimization decision-making. It significantly propels the transformation of tunnel construction from traditional extensive management toward data-driven, refined, and intelligent paradigms. Future research efforts will focus on the following two directions: First, incorporating the mechanical structural constraints of the trolley itself (e.g., maximum allowable deformation) into the optimization model to ensure the practical feasibility of pose adjustments. Second, exploring the integration of this optimization algorithm with automatic total station guidance systems to achieve real-time, closed-loop automated control of trolley positioning.

REFERENCES

Agarwal, S., Mierle, K., Team, T.C.S., 2023. Ceres solver.

Ghorbani, M., Shahriar, K., Sharifzadeh, M., Masoudi, R., 2020. A critical review on the developments of rock support systems in high stress ground conditions. Int. J. Min. Sci. Technol. 30, 555–572. https://doi.org/10.1016/j.ijmst.2020.06.002

Hosamo, H.H., Hosamo, M.H., 2022. Digital Twin Technology for Bridge Maintenance using 3D Laser Scanning: A Review. Adv. Civ. Eng. 2022, 2194949. https://doi.org/10.1155/2022/2194949

Kang, Z., Zhang, L., Tuo, L., Wang, B., Chen, J., 2014. Continuous extraction of subway tunnel cross sections based on terrestrial point clouds. Remote Sens. 6, 857–879.

Khudhair, A., Li, H., Ren, G., Liu, S., 2021. Towards future BIM technology innovations: A bibliometric analysis of the literature. Appl. Sci. 11, 1232.

Manzoor, B., Othman, I., Pomares, J.C., 2021. Digital technologies in the architecture, engineering and construction (Aec) industry—a bibliometric—qualitative literature review of research activities. Int. J. Environ. Res. Public. Health 18, 6135.

Merisalu, J., Sundell, J., Rosen, L., 2023. Probabilistic cost-benefit analysis for mitigating hydrogeological risks in underground construction. Tunn. Undergr. Space Technol. 131, 104815.

Shen, X., Lu, M., Fernando, S., AbouRizk, S.M., 2012. Tunnel boring machine positioning automation in tunnel construction, in: ISARC. Proceedings of the International Symposium on Automation and Robotics in Construction. IAARC Publications, p. 1.
Suárez-Fino, J.F., Mayoral, J.M., 2024. Numerical Modeling for Tunnel Lining Optimization. Appl. Sci. 14, 7415.
Xie, X., Zhao, M., He, J., Zhou, B., 2018. Automatic Processing Method for Deformation Monitoring of Circle Tunnels Based on 3D LiDAR Data.
Zhi, Z., Chang, B., Li, Y., Du, Z., Zhao, Y., Cui, X., Ran, J., Li, A., Zhang, W., 2025. P-CSF: Polar coordinate cloth simulation filtering algorithm for multi-type tunnel point clouds. Tunn. Undergr. Space Technol. 155, 106144.
Zhou, Z., Zhu, X., Zheng, C., Zhang, Z., Zhang, H., Zhou, Z., Zhu, X., Zheng, C., Zhang, Z., Zhang, H., 2023. The Optimization of Waterproof and Drainage Design and an Evaluation of the Structural Safety of Tunnels in Weak Watery Strata. Buildings 13. https://doi.org/10.3390/buildings13102499

BIOGRAPHICAL NOTES

Bingtao Chang received the B.E. and M.Sc. degrees from the Shandong University of Science and Technology, Qingdao, China, in 2018 and 2021, respectively. He is currently pursuing the Ph.D. degree with the School of Geospatial Engineering and Science, Sun Yat-sen University, Zhuhai, China. His research topic is LiDAR point cloud processing.

Wuming Zhang received the Ph.D. degree from Tsinghua University, Beijing, China, in 2004. He is currently a Professor with the School of Geospatial Engineering and Science, Sun Yat-sen University, Zhuhai, China. His research interests include photogrammetry and remote sensing, especially light detection and ranging (LiDAR) point cloud processing and applications.

CONTACTS

Wuming Zhang
School of Geospatial Engineering and Science, Sun Yat-sen University
Zhuhai
China
Tel. +86-13671141927
Email: zhangwm25@mail.sysu.edu.cn